Monitoring fibril formation of the N-terminal domain of PABPN1 carrying an alanine repeat by tryptophan fluorescence and real-time NMR

ARTICLE *in* FEBS LETTERS · JUNE 2008

Impact Factor: 3.17 · DOI: 10.1016/j.febslet.2008.04.002 · Source: PubMed

6 AUTHORS, INCLUDING:

Julia Rohrberg
University of California, San Francisco
6 PUBLICATIONS **148** CITATIONS
SEE PROFILE

Mirko Sackewitz
Novartis
7 PUBLICATIONS **84** CITATIONS
SEE PROFILE

Jochen Balbach
Martin Luther University Halle-Wittenberg
104 PUBLICATIONS **2,153** CITATIONS
SEE PROFILE

FEBS Letters 582 (2008) 1587–1592

Monitoring fibril formation of the N-terminal domain of PABPN1 carrying an alanine repeat by tryptophan fluorescence and real-time NMR

Julia Rohrberg[a,1], Rolf Sachs[b], Grit Lodderstedt[a,2], Mirko Sackewitz[a], Jochen Balbach[b], Elisabeth Schwarz[a,*]

[a] *Institute for Biochemistry and Biotechnology of the Martin-Luther-University Halle-Wittenberg, Kurt-Mothes-Strasse 3, 06120 Halle, Germany*
[b] *Institute of Physics, Biophysics Group and "Mitteldeutsches Zentrum für Struktur und Dynamik der Proteine, MZP" of the Martin-Luther-University Halle-Wittenberg, Hoher Weg 8, 06120 Halle, Germany*

Received 20 February 2008; revised 2 April 2008; accepted 2 April 2008

Available online 10 April 2008

Edited by Jesus Avila

Abstract **Intranuclear fibrils due to poly-alanine expansions in the N-terminal domain of the poly(A) binding protein PABPN1 correlate with the disease oculopharyngeal muscular dystrophy (OPMD). For monitoring fibril formation by fluorescence and real-time NMR spectroscopy, tryptophans were introduced either into the middle or C-terminal of the poly-alanine segment. The kinetics of fibril formation which were monitored by fluorescence spectroscopy were matched by real-time NMR kinetics. Our results show that fibril formation is concomitant with the burial of the tryptophans in the fibrillar core. Since no soluble pre-fibrillar intermediate(s) was detected, fibril formation of this domain may be regarded as a two state conversion from an unfolded soluble into folded insoluble species.**

Keywords: Poly-alanine; PABPN1; Fibril formation; Real-time NMR; Tryptophan fluorescence; Trinucleotide expansion

1. Introduction

Oculopharyngeal muscular dystrophy (OPMD) is a late onset disease due to trinucleotide or codon expansions in the gene for the nuclear poly(A) binding protein, PABPN1, which controls mRNA poly-adenylation [1,2]. OPMD symptoms are eye lid drooping, swallowing difficulties and proximal limb weakness, with the swallowing difficulties being usually the major impairment. The disease is characterized by amyloid-like intranuclear deposits consisting mainly of PABPN1 [3–6]. On the level of the translation product, the codon expansions result in the extension of a poly-alanine stretch which is directly positioned after the start methionine. In healthy individuals a stretch of 10 alanine residues is observed, in OPMD patients the homo-oligo-alanine segment can be expanded to maximally 17 alanine residues [7].

The in vitro analysis of amyloid-like deposit formation, as it is observed in patient tissue, has so far been hampered by the propensity of the full length protein to form non-fibrillar, amorphous aggregates. These aggregates most likely form because of the oppositely charged terminal domains independently of the presence or absence of alanine extensions [8]. Therefore, in vitro fibril formation was studied with the N-terminal domain of PABPN1. The analyses revealed that also the N-terminal domain of PABPN1 possessing the wild type (N-WT) alanine segment of 10 residues forms fibrils. However, shorter lag phases and faster elongation rates were obtained with the domain containing the most extreme extension observed in human, seven additional alanines (N-(+7)Ala) [8,9]. Furthermore, fibrils of N-WT and N-(+7)Ala differ in their morphology and resistance against solubilization [8,9].

The N-terminal domain of PABPN1 comprising 125 amino acids lacks tertiary contacts both in its natural context of the full-length protein and in the isolated form [10]. Recent investigations by solid state NMR of the structure of fibrils formed by N-(+7)Ala suggest that the poly-alanine segment is rigid in the fibrils (Sackewitz et al., submitted for publication). However, so far, no information exists about the structural transition(s) which take place in the N-terminal domain during conversion from the soluble to the fibrillar state. Monitoring fibril formation of the N-terminal domain N-(+7)Ala by fluorescence spectroscopy is not possible because of the lack of tryptophans. Thus, for the analysis of fibril formation, tryptophan residues were introduced into and C-terminal of the poly-alanine segment. Tryptophan fluorescence studies have proven valuable approaches in analyses of fibril formation: Insertions of tryptophans at different positions of the Aβ peptide enabled fluorescence studies during conversion from the soluble to the fibrillar state [11]. Tryptophan mutants (Y39W) of α-synuclein [12] and β2-microglobulin [13] allowed as well comprehensive analyses of fibril formation processes.

The tryptophan insertions into N-(+7)Ala allowed monitoring fibril formation by fluorescence spectroscopy. Shifts of tryptophan fluorescence maxima were paralleled by the kinetics of the decrease in acrylamide quench indicating that the tryptophans become buried in a folded structure upon fibril

*Corresponding author. Fax: +49 345 55 27 013.
E-mail address: Elisabeth.Schwarz@biochemtech.uni-halle.de (E. Schwarz).

[1]Present address: Technical University Munich, Institute for Organic Chemistry and Biochemistry, Lichtenbergstrasse 4, 85747 Garching, Germany.
[2]Present address: Scil Proteins GmbH, Heinrich-Damerow-Strasse 1, 06120 Halle, Germany.

0014-5793/$34.00
doi:10.1016/j.febslet.2008.04.002

formation. The kinetics observed by fluorescence spectroscopy were matched by real-time NMR measurements in which the disappearance of the tryptophan peak over time was used as a tool to follow fibril formation. Taken together, our results indicate that fibril formation of N-(+7)Ala can be described as a two state conversion of a poorly structured or even natively unfolded protein domain into the stably folded fibril without the existence of soluble pre-fibrillar intermediates.

2. Materials and methods

2.1. Recombinant expression constructs

For recombinant production in *Escherichia coli* cells, DNA coding for the N-terminal fragment of PABPN1 with seven additional alanine residues was expressed via pET15b, a vector which provides an N-terminal His-tag [8,9]. Tryptophan residues were introduced via the QuikChange mutagenesis kit (Stratagene). For introducing the tryptophan residue at position 11 (counted from the start methionine of the naturally occurring protein with an alanine extension) primer 5′-GCG GCG GCA GCG GCA GCA TGG GCG GCG GCA GCA GCA GCA-3′, and for insertion at position 22, primer 5′-GCA GCA GCA GGA GCA GCA TGG GGA GGA AGA GGA TCA GGA-3′ and the complementary primers were used. The mutant constructs were verified by DNA sequencing.

2.2. Fibril formation and fibril analysis

Fibrils were allowed to form at a protein concentration of 1 mM at 37 °C in fibrillation buffer (5 mM KH_2PO_4, 150 mM NaCl, pH 7.4). Fibril formation was monitored by ANS fluorescence as described [9]. Not-fibrillized protein was separated from fibrillar species by centrifugation for 1 h at 70,000 rpm. The supernatant was removed and analysed immediately, the pellet was washed twice and resuspended in the original volume of fibrillation buffer.

2.3. Far UV circular dichroism (CD) and fluorescence measurements

CD spectra were recorded at 20 °C on a Jasco J-810 CD-spectrometer. Measurements were performed in 0.1 mm quartz cuvettes at a protein concentration of 1 mg/ml in fibrillation buffer. Excitation and emission slit widths were 1 nm, the integration time was 1 s with an increment of 1.0 nm. Spectra represent averages of seven scans and are buffer-corrected. For fluorescence measurements aliquots (4 μl) of the washed and resuspended fibril pellet, the supernatant or the total fibril sample were added to 800 μl fibrillation buffer. Fluorescence spectra were recorded on a Jobin Yvon Spex Fluoromax 2 at 20 °C upon excitation at 295 nm. Experiments were performed in 1 cm quartz cuvettes with excitation and emission slit widths of 5 nm, an integration time of 0.2 s and an increment of 1.0 nm. Spectra represent averages of three scans and are buffer-corrected. To define the fluorescence maxima, weibull five parameters were fit in sigma plot to the spectra. Fits with $R^2 > 0.9$ were used for fluorescence maximum determination.

2.4. Acrylamide quenching

Not-fibrillized protein was separated from fibrillar species by centrifugation. Aliquots of the supernatant or of resuspended fibrils were added to 800 μl fibrillation buffer to final concentrations of 5 μM. Subsequently, acrylamide was added to the samples at the indicated final concentrations. The intrinsic fluorescence was recorded in absence (I_0) and presence (I) of the quencher and I_0/I plotted against acrylamide concentration (Stern–Volmer plots). For monitoring fluorescence quenching by acrylamide during fibrillation, aliquots of the samples were removed at the indicated time points and diluted into freshly prepared fibrillation buffer containing 0.625 M acrylamide. The protein concentration was 5 μM. Intrinsic fluorescence signals were recorded in the absence (I_0) and presence (I) of the quencher and the ratio I_0/I was plotted against the incubation time. Quenching was monitored by emission signals at 350 nm upon excitation at 295 nm.

2.5. NMR spectroscopy

Proton spectra of W(22)-N-(+7)Ala were recorded at 37 °C on a Bruker Avance II 600 spectrometer. The fibril formation kinetics were measured in fibrillation buffer with 1% (w/v) NaN_3 in 90% H_2O/10% D_2O. Eight hundred and sixty one-dimensional (1D) ^1H spectra were acquired over 110 h. Two further spectra were recorded after 400 and 615 h. The solvent resonance was suppressed by WATERGATE. Data were processed and analysed using Felix 2.1. Several spectral regions (0.7–1.0, 7.3–8.7, 10.1 ppm) were integrated and plotted against the incubation time.

2.6. Miscellaneous

Recombinant protein expression and purification, electron microscopy and monitoring fibril formation kinetics were performed as described [9].

3. Results

3.1. Tryptophan insertions do not interfere with fibril formation of N-(+7)Ala

Tryptophan residues were introduced into N-(+7)Ala to generate chromophores which are sensitive to the polypeptide environment and should thereby allow recording of the fibrillation process by fluorescence spectroscopy. Since it was not clear whether the insertion of tryptophans would interfere with fibrillation, two insertion mutants were produced, W(11)-N-(+7)Ala in which the tryptophan was in the middle of the oligo-alanine segment and W(22)-N-(+7)Ala with the chromophore at a C-terminal position of the alanine stretch (Fig. 1A). After recombinant production and purification, secondary structural elements of the insertion variants were examined by far UV CD spectroscopy and compared to those of N-

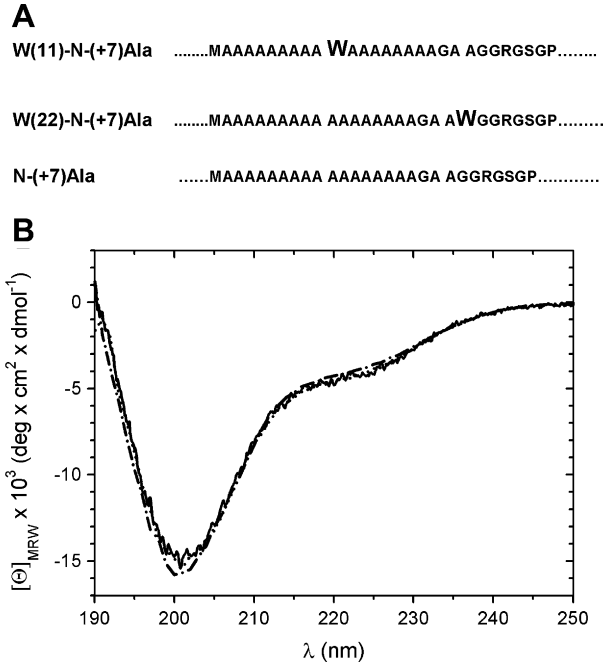

Fig. 1. (A) Scheme of the positions of the tryptophan insertions in the N-terminal domain of PABPN1 with seven additional alanines and for comparison, the naturally occurring N-terminal domain with the alanine extensions, N-(+7)Ala. (B) Far UV CD analysis of the soluble variants. Far UV CD spectra of W(11)-N-(+7)Ala (dashed-dotted line), W(22)-N-(+7)Ala (dotted line) and N-(+7)Ala (solid line) were recorded as described in Section 2.

(+7)Ala (Fig. 1B). The spectra of all three constructs are superimposable demonstrating that the tryptophan neither in the middle nor in the C-terminal position of the alanine stretch causes a significant change in the secondary structural elements.

Next, fibril formation of W(11)-N-(+7)Ala and W(22)-N-(+7)Ala was investigated by monitoring increases of ANS fluorescence. Unexpectedly, fibril formation of the variants proceeded with faster elongation rates and shorter lag phases than observed for N-(+7)Ala (Fig. 2A). The presence of amyloid-like structures was confirmed by electron microscopy. The fibrils of both variants showed unbranched structures similar to those formed by N-(+7)Ala (Fig. 2B and C).

3.2. Solvent exposure of the tryptophan residues changes upon fibril formation

In order to detect changes in solvent accessibility of the tryptophan residues upon fibril formation, fluorescence spectra of W(11)-N-(+7)Ala and W(22)-N-(+7)Ala were recorded during fibrillation and the fluorescence maxima were determined (Fig. 3). At early time points, the maximum of the fluorescence peak was at 358 nm indicating solvent exposure of the tryptophan residues as it is expected with a protein domain lacking defined tertiary contacts [14]. Upon prolonged incubation, substantial blue shifts from 358 to 345 nm were observed. Additionally, time-dependent increases in fluorescence intensities at the new fluorescence maxima at 345 nm were detected, which correlated with the increases in ANS fluorescence (Fig. 2A). The blue shifts of fluorescence maxima and the increases of fluorescence signals were interpreted by increases in the hydrophobicity of tryptophan environment and burial of these residues upon fibrillation.

To analyse monomers and fibrils separately, aliquots were removed after various incubation intervals. The samples were centrifuged, and supernatants (monomers) and resuspended pellets (fibrils) were analysed by fluorescence spectroscopy. The fluorescence emission maxima of the supernatant and pellet fraction remained constant at 358 nm and 345/344 nm, respectively (Fig. 4A). The data show that via fluorescence spectroscopy, the monomeric species can be discriminated from the fibrillar species. The stable fluorescence maxima for

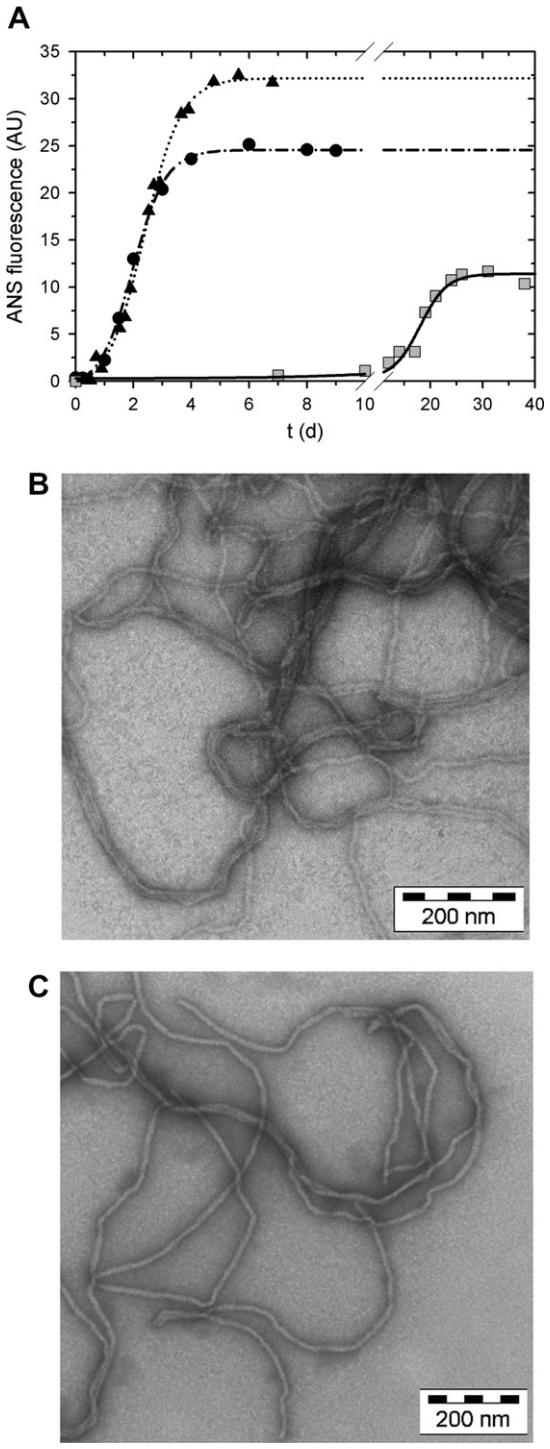

Fig. 2. Fibril formation of the two tryptophan insertion mutants and N-(+7)Ala. (A) Kinetics of fibril formation of W(11)-N-(+7)Ala (circles, dashed-dotted line) and W(22)-N-(+7)Ala (triangles, dotted line) in comparison with N-(+7)Ala (squares, solid line). Fibril formation was monitored by ANS fluorescence. Sigmoidal curves were fitted to the fluorescence intensities. (B) Electron micrograph of fibrils formed by W(11)-N-(+7)Ala after 9 days and (C) W(22)-N-(+7)Ala after 13 days of incubation.

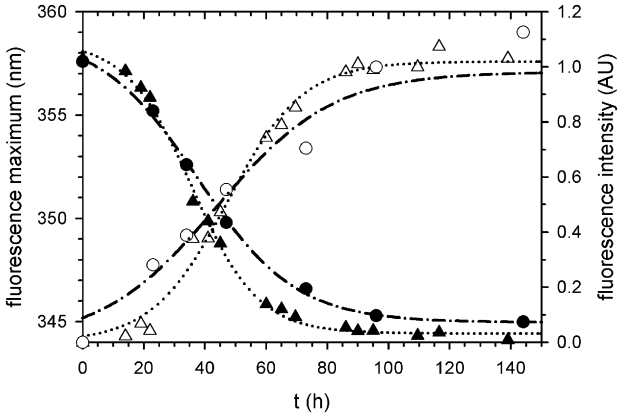

Fig. 3. Time-dependent changes of the spectroscopic properties of the tryptophan insertion variants. Blue shifts of tryptophan fluorescence maxima of W(11)-N-(+7)Ala (black circles, dotted-dashed line) and W(22)-N-(+7)Ala (black triangles, dotted line) are indicated on the left ordinate. Increases of tryptophan fluorescence intensities at 344/345 nm of W(11)-N-(+7)Ala (open circles, dotted-dashed line) and W(22)-N-(+7)Ala (open triangles, dotted line) are shown on the right ordinate. Curves were fitted to obtain sigmoidal shapes.

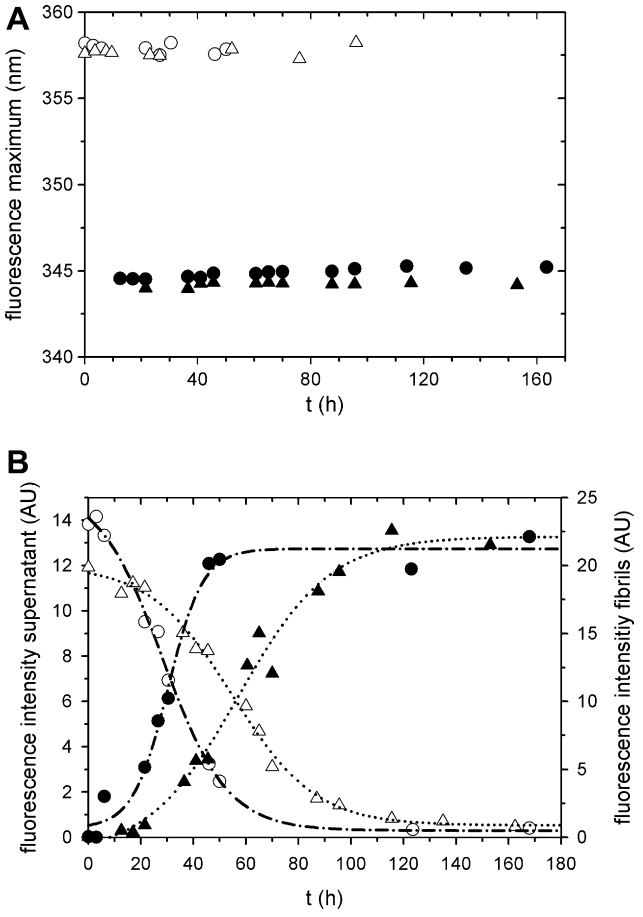

Fig. 4. Changes in the intrinsic tryptophan fluorescence of the separated monomeric and fibrillar species. (A) Plot of the tryptophan fluorescence maximum versus the incubation time of W(11)-N-(+7)Ala, supernatant (open circles), fibrils (closed circles). Tryptophan fluorescence signals of W(22)-N-(+7)Ala, supernatant (open triangles), fibrils (closed triangles). (B) Time-dependent decrease of the tryptophan fluorescence intensities in the soluble fraction, W(11)-N-(+7)Ala (open circles, dashed-dotted line) and W(22)-N-(+7)Ala (open triangles, dotted line) at 358 nm and increases of intensities in the fibrils (W(11)-N-(+7)Ala, closed circles; W(22)-N-(+7)Ala, triangles) at 345, 344 nm. Curves were plotted to obtain sigmoidal shapes.

the two species indicate no significant alteration in the tryptophan environment. The time-dependent decrease of the fluorescence intensity of the soluble species at 358 nm corresponded to the increase of fluorescence intensity at 344/345 nm of the insoluble fraction (Fig. 4B). Thus, a direct conversion of the soluble protein into fibrillar species without soluble intermediate states can be envisaged.

3.3. Acrylamide quenching of tryptophan fluorescence decreases during fibril formation

Solvent accessibility of the tryptophans was measured by acrylamide quenching. First the acrylamide concentration which was required for quenching was determined by adding increasing concentrations of acrylamide to monomeric and fibrillar fractions. The concentration-dependent fluorescence quench of the soluble species was visualized by Stern–Volmer plots (Fig. 5A). In contrast to the soluble species, the fibrillar fractions of both tryptophan variants did not display a significant fluorescence quench indicating that the tryptophans are

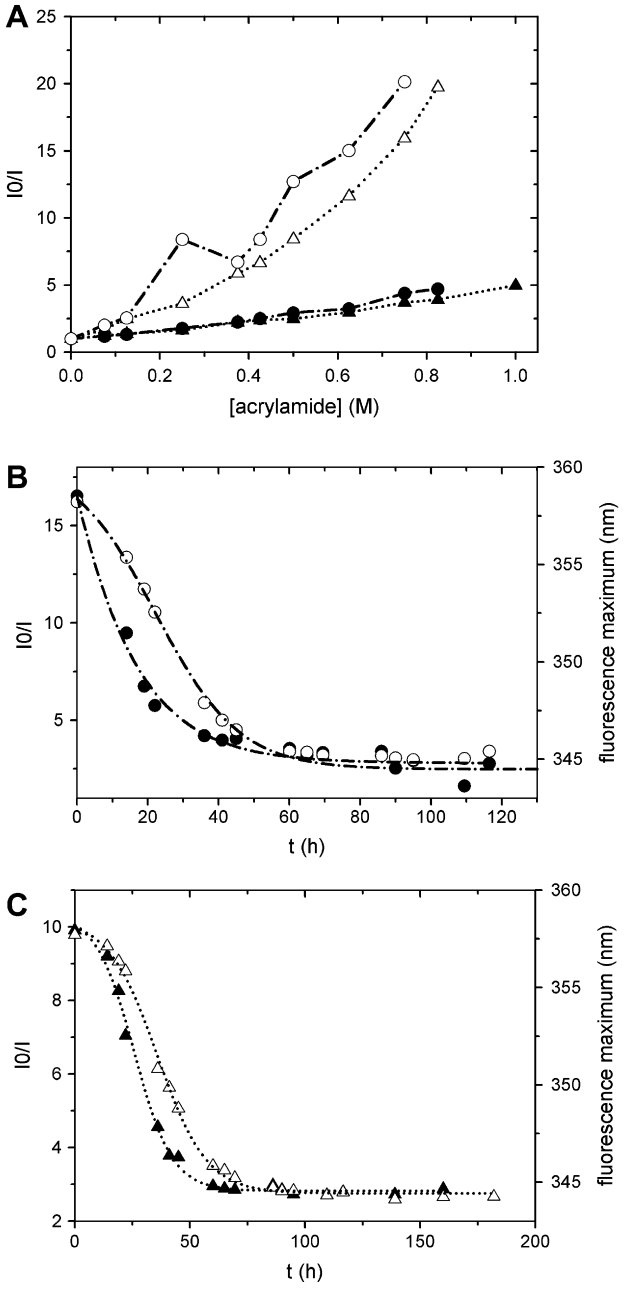

Fig. 5. Fluorescence quench by acrylamide. (A) The ratio of tryptophan fluorescence at 350 nm in absence (I_0) and presence (I) of acrylamide was plotted against increasing concentrations of acrylamide. Fibrils (closed symbols) and soluble protein (open symbols) of W(11)-N-(+7)Ala (circles, dotted-dashed lines) and W(22)-N-(+7)Ala (triangles, dotted lines). (B) and (C) Time-dependent decreases of I_0/I and fluorescence maxima of W(11)-N-(+7)Ala (closed circles) (B) and W(22)-N-(+7)Ala (closed triangles) (C). Shifts of fluorescence maxima are indicated by the open symbols. Fluorescence quenching by acrylamide was analysed at 350 nm and an acrylamide concentration of 0.625 M. All curves were fitted for sigmoidal shapes.

no longer solvent exposed in the fibrils. Thus, fibrillation kinetics were monitored by acrylamide quenching analysis. The time-dependent changes in fluorescence quenches were analysed in the presence of 0.625 M acrylamide (Fig. 5B and C). The kinetics of the reduction in the acrylamide quenches correlate roughly with the slightly delayed kinetics of tryptophan blue shifts.

3.4. ^1H NMR resonances monitor site-specifically the fibril formation

For detailed investigations of the structural changes in W(22)-N-(+7)Ala during fibril formation, a time resolved NMR experiment was performed. Liquid state NMR allows only to detect ^1H resonances of protein protons, if the polypeptide chain tumbles fast enough to average out the dipolar couplings. This is the case for all protons of W(22)-N-(+7)Ala at a monomeric or low oligomeric state and for protons of the chains, which stick out from the fibrils into the solution. This structural information is converse to solid state NMR analyses employing cross-polarization, where only resonances are detectable for nuclei with restricted motions inside the fibrils (Sackewitz et al., submitted for publication). In the real-time NMR experiment presented here, 860 1D ^1H NMR spectra in solution were recorded during 615 h of fibrillation (Fig. 6A). The first 1D ^1H NMR spectrum of W(22)-N-(+7)Ala recorded immediately after initiation of the fibrillation reaction by dissolving the protein, resembles very closely that of N-(+7)Ala [10] with an additional, well resolved resonance at 10.1 ppm from the $H^{\varepsilon 1}$ proton of the tryptophan side chain. It represents the spectrum of a fully unfolded protein. To follow the time course of different resonances, the spectral regions of methylene/methyl groups, amides and the $H^{\varepsilon 1}$ proton were integrated and plotted against the incubation time (Fig. 6B). All kinetics show a lag phase of ca. 50 h followed by an exponential decay. The integrals decay, because the number of soluble, fast tumbling protein molecules decreases. This time course is consistent with the fibril formation experiments followed by ANS fluorescence. Interesting is the appearance of the last ^1H NMR spectrum after the fibrillation had finished. The signal of the tryptophan side chain disappeared almost completely (Fig. 6A and B), whereas amide and methylene/methyl protons show remaining signals with ca. 20% of the initial integral value. These data suggest that the tryptophan residue of W(22)-N-(+7)Ala is positioned closely to the poly-alanine stretch, which forms the core of the fibril and therefore restricts the local motions. The remaining signals belong to C-terminal part of the polypeptide chains sticking out into the solution with sufficient flexibility.

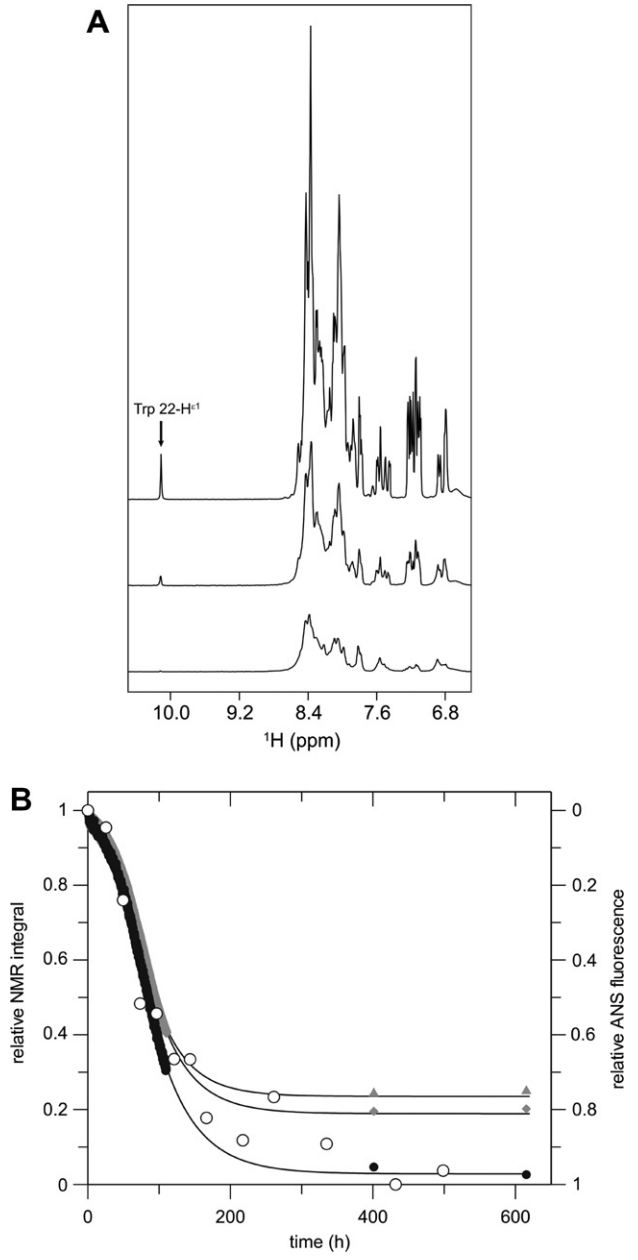

Fig. 6. Real-time NMR analysis of fibril formation of W(22)-N-(+7)Ala. (A) Low field sections of 1D ^1H NMR spectra of W(22)-N-(+7)Ala at the beginning (top), after 110 h (middle), and at the end of the fibrillation experiment (bottom) at 37 °C. (B) Decay of 1D ^1H NMR resonances of W(22)-N-(+7)Ala during fibril formation. Relative NMR integrals of the amide region (triangles, 7.3–8.7 ppm), methylene/methyl group region (diamonds, 0.7–1.0 ppm) and the single tryptophan side chain resonance (closed circles, 10.1 ppm). For the decrease of NMR integrals, a single exponential function between 75 and 620 h was assumed (solid lines). Open circles represent the relative ANS fluorescence increase according to Fig. 2A using inverse *y*-scaling.

4. Discussion

Mutational approaches have proven useful tools to probe amyloid formation [12,13,15,16]. Though the exchanges are likely to modify certain facets of the molecular transitions during fibril formation and the fibril structure itself, this approach is legitimated by the occurrence of natural exchanges in amyloidogenic proteins or their peptides such as Alzheimer peptide or α-synuclein [17–19].

Here, fibril formation of the N-terminal domain of PABPN1 was monitored with tryptophan insertion mutants. The tryptophan residues which had been introduced into the poly-alanine segment did not suppress fibril formation, rather fibril formation was accelerated, a fact that could be explained by the high hydrophobicity of tryptophans and their propensity to form β-strands [20]. Thus, the tryptophans could lower activation energies from the soluble to the insoluble state. Though non-fibrillar, oligomeric deposits of the tryptophan variants have been never observed by electron microscopy, we cannot completely exclude the unlikely existence of insoluble intermediate(s).

Since after fibril formation fluorescence blue shifts were observed and acrylamide quenching was no longer detectable, the tryptophans must be integrated into the β-core structure of the fibrils. Of course, on the atomic level, the fibrillar structures of both tryptophan insertion variants are presumably different from those of N-(+7)Ala due to the packing of the large

aromatic side chain into the β-strands. Since fibrils formed by N-(+7)Ala and the wild type fragment containing 10 alanine residues differ in their morphology and chemical properties [9], differences between fibrils of the tryptophan insertion variants and the unaltered N-terminal domain are to be expected. Nevertheless, the tryptophan insertions allowed characterization of the fibril formation process by fluorescence spectroscopy and by real-time NMR. Both techniques show that the tryptophans at position 11 and 22 are part of the β-cross structure of the fibrils and they are not solvent-accessible anymore. This result confirms earlier findings of our group which indicate that the poly-alanine segment is rigid and protease-protected in the fibrils (Sackewitz et al., submitted for publication). Fibril formation kinetics detected by real-time NMR matched those recorded by the fluorescence approach. However, via real-time NMR, a considerably more accurate description of the conversion kinetics is possible than by the fluorescence studies. The NMR kinetic data indicate that no soluble kinetic intermediate(s) is populated during fibrillation. Furthermore, in several preliminary experiments, fibril formation was monitored by real-time NMR with natural N-(+7)Ala lacking the tryptophan insertion (data not shown). However, for these studies fibril formation had to be seeded, since unseeded fibrillation required measurements of approx. 20–30 days. Also with these seeded samples, biphasic signal decays, which would indicate a soluble intermediate have never been detected.

Taken together, these results imply that fibril formation of the N-terminal domain of PABPN1 does not resemble that of α-synuclein, which also slowly converts from a natively unfolded structure into amyloid-like fibrils, however, via the transient formation of non-fibrillar oligomeric structures [21].

Acknowledgements: This work was funded by the Deutsche Forschungsgemeinschaft DFG through SFB 610 and GRK 1026.

References

[1] Wahle, E. and Ruegsegger, U. (1999) 3′-End processing of pre-mRNA in eukaryotes. FEMS Microbiol. Rev. 23, 277–295.
[2] Wahle, E. (1991) A novel poly(A)-binding protein acts as a specificity factor in the second phase of messenger RNA polyadenylation. Cell 66, 759–768.
[3] Tome, F.M., Chateau, D., Helbling-Leclerc, A. and Fardeau, M. (1997) Morphological changes in muscle fibers in oculopharyngeal muscular dystrophy. Neuromuscul. Disord. 7 (Suppl. 1), S63–S69.
[4] Tome, F.M. and Fardeau, M. (1980) Nuclear inclusions in oculopharyngeal dystrophy. Acta Neuropathol. (Berl.) 49, 85–87.
[5] Calado, A., Tome, F.M., Brais, B., Rouleau, G.A., Kuhn, U., Wahle, E. and Carmo-Fonseca, M. (2000) Nuclear inclusions in oculopharyngeal muscular dystrophy consist of poly(A) binding protein 2 aggregates which sequester poly(A) RNA. Hum. Mol. Genet. 9, 2321–2328.
[6] Uyama, E., Tsukahara, T., Goto, K., Kurano, Y., Ogawa, M., Kim, Y.J., Uchino, M. and Arahata, K. (2000) Nuclear accumulation of expanded PABP2 gene product in oculopharyngeal muscular dystrophy. Muscle Nerve 23, 1549–1554.
[7] Brais, B. et al. (1998) Short GCG expansions in the PABP2 gene cause oculopharyngeal muscular dystrophy. Nat. Genet. 18, 164–167.
[8] Scheuermann, T., Schulz, B., Blume, A., Wahle, E., Rudolph, R. and Schwarz, E. (2003) Trinucleotide expansions leading to an extended poly-L-alanine segment in the poly (A) binding protein PABPN1 cause fibril formation. Protein Sci. 12, 2685–2692.
[9] Lodderstedt, G., Hess, S., Hause, G., Scheuermann, T., Scheibel, T. and Schwarz, E. (2007) Effect of oculopharyngeal muscular dystrophy-associated extension of seven alanines on the fibrillation properties of the N-terminal domain of PABPN1. FEBS J. 274, 346–355.
[10] Lodderstedt, G. et al. (2008) Hofmeister salts and potential therapeutic compounds accelerate in vitro fibril formation of the N-terminal domain of PABPN1 containing a disease-causing alanine extension. Biochemistry 47, 2181–2189.
[11] Garzon-Rodriguez, W., Vega, A., Sepulveda-Becerra, M., Milton, S., Johnson, D.A., Yatsimirsky, A.K. and Glabe, C.G. (2000) A conformation change in the carboxyl terminus of Alzheimer's Abeta (1–40) accompanies the transition from dimer to fibril as revealed by fluorescence quenching analysis. J. Biol. Chem. 275, 22645–22649.
[12] Dusa, A., Kaylor, J., Edridge, S., Bodner, N., Hong, D.P. and Fink, A.L. (2006) Characterization of oligomers during alpha-synuclein aggregation using intrinsic tryptophan fluorescence. Biochemistry 45, 2752–2760.
[13] Kihara, M., Chatani, E., Iwata, K., Yamamoto, K., Matsuura, T., Nakagawa, A., Naiki, H. and Goto, Y. (2006) Conformation of amyloid fibrils of beta2-microglobulin probed by tryptophan mutagenesis. J. Biol. Chem. 281, 31061–31069.
[14] Schmid, F.X. (1997) Spectral methods of characterizing protein conformation and conformational changes in: Protein Structure: A Practical Approach (Creighton, T.E., Ed.), pp. 251–285, IRL-Press/Oxford University Press, Oxford/New York/Tokio.
[15] Williams, A.D., Portelius, E., Kheterpal, I., Guo, J.T., Cook, K.D., Xu, Y. and Wetzel, R. (2004) Mapping abeta amyloid fibril secondary structure using scanning proline mutagenesis. J. Mol. Biol. 335, 833–842.
[16] Williams, A.D., Shivaprasad, S. and Wetzel, R. (2006) Alanine scanning mutagenesis of Abeta(1–40) amyloid fibril stability. J. Mol. Biol. 357, 1283–1294.
[17] Meinhardt, J. et al. (2007) Similarities in the thermodynamics and kinetics of aggregation of disease-related Abeta(1–40) peptides. Protein Sci. 16, 1214–1222.
[18] Thomas, B. and Beal, M.F. (2007) Parkinson's disease. Hum. Mol. Genet. 16 (Spec. No. 2), R183–R194.
[19] Fredenburg, R.A., Rospigliosi, C., Meray, R.K., Kessler, J.C., Lashuel, H.A., Eliezer, D. and Lansbury Jr., P.T. (2007) The impact of the E46K mutation on the properties of alpha-synuclein in its monomeric and oligomeric states. Biochemistry 46, 7107–7118.
[20] Chou, P.Y. and Fasman, G.D. (1974) Conformational parameters for amino acids in helical, beta-sheet, and random coil regions calculated from proteins. Biochemistry 13, 211–222.
[21] Rochet, J.C., Conway, K.A. and Lansbury Jr., P.T. (2000) Inhibition of fibrillization and accumulation of prefibrillar oligomers in mixtures of human and mouse alpha-synuclein. Biochemistry 39, 10619–10626.